Emulation Design for a Class of Extremum Seeking Controllers: Case Studies in ABS Design and Spark Timing Calibration

Alireza Mohammadi, Dragan Nešić and Chris Manzie

***Abstract*— The vast majority of extremum seeking designs in the literature are in continuous-time, however their practical implementation is typically done using digital technology. In this paper, a sampled-data implementation of extremum seeking controllers using emulation design methods is studied to address this gap. The conditions under which the emulated controller preserves the performance of the continuous-time plant are investigated. The main result also provides a guideline on how to tune the controller parameters including sample period in order to achieve the desired performance. The examples of anti-lock braking and spark timing calibration are used to illustrate the proposed design method through simulation and experimental tests.**

I. Introduction

Extremum seeking (ES) is an online approach with the goal of optimizing the system output, using little or no information about the plant. Since an ES controller does not need the exact model of the plant and also can easily deal with multi input systems, it has been successfully used in a range of applications [8].

Most ES developments are in continuous-time, despite the fact that almost all practical implementations are effectively discrete-time. While there exist a few results in discrete-time ES control [3],[6], the stability analysis is quite different from that of continuous-time and therefore most useful tools like averaging and singular perturbation cannot be directly used in stability analysis [2]. This has led to a mismatch in the major theoretical ES developments and their practical implementation on real-world systems.

This paper takes advantage of emulation design methods to port the existing continuous-time methods to discrete-time frameworks. Emulation of a system consists of two steps: (1) the design of a continuous-time controller for a continuous-time plant using known continuous-time design methods to satisfy closed-loop control performance objectives, and (2) the discretization and implementation of the continuous-time controller using sample and hold devices with the objective of obtaining comparable closed-loop system properties [11]. Emulation control of nonlinear systems has been widely investigated in the literature [13],[14]. However, due to the singularly perturbed structure of the ES schemes, the existing results cannot be used directly. Moreover, due to the time scale separation required for averaging and singular perturbation in stability analysis of continuous-time ES controllers, some parameters should be tuned appropriately in the closed-loop system. The emulation design method also introduces sample period as additional tuning parameter.

The first objective of this paper is to develop a tuning procedure for controller parameters including sample period to ensure that the discretized controller preserves the closed-loop performance of the continuous-time controller under sampling. This paper deals with a class of ES controllers whereby a known plant structure with uncertain parameters has been used in the online optimization of the plant operation [1], [9]. Since known information about the model structure is incorporated in the closed-loop system, it is referred to as a grey-box ES approach.

The second objective of the paper is to demonstrate the ability and flexibility of the proposed discrete-time ES framework through simulations for anti-lock braking system to regulate the wheel longitudinal slip to the maximum point of the friction curve in order to generate the maximum braking force; and in a practical situation to find the optimum spark-timing that gives the maximum brake torque in a natural gas fueled engine.

The paper is organized as follows. The framework for continuous-time grey-box ES controllers is presented in Sections II followed by its emulation design in Section III. Section IV demonstrates the application of the main results through simulation studies to anti-lock braking problem and through experiments for spark timing calibration. Conclusions are presented in Section V, followed by the proof of the main result in the Appendix.

Notation: The set of real numbers is denoted by $\mathbb{R}$. The continuous function $\alpha : [0, a) \to \mathbb{R}_{\geq 0}$ is said to belong to class $\mathcal{K}$ if it is nondecreasing and zero at zero. The continuous function $\alpha : \mathbb{R}_{\geq 0} \to \mathbb{R}_{\geq 0}$ is said to be of class $\mathcal{K}_\infty$ if it is strictly increasing, unbounded and zero at zero.

II. The Framework for Continuous-Time Grey-box ES Controllers

Consider the continuous-time closed-loop system with a nonlinear dynamic plant [9]:

$$\dot{x} = f(\theta, x, u) , \tag{1}$$
$$y = Q(\theta, x) , \tag{2}$$
$$u = \xi + d(\epsilon_1 t) , \tag{3}$$
$$\dot{\hat{\theta}} = \epsilon_1 \, G(\hat{\theta}, \eta, y, u) , \tag{4a}$$
$$\dot{\eta} = \epsilon_1 \, H(\eta, y, u) , \tag{4b}$$
$$\dot{\xi} = \epsilon_1 \, \epsilon_2 \, F(\hat{\theta}, \xi), \qquad \epsilon_1, \, \epsilon_2 > 0, \tag{5}$$

where $x \in \mathbb{R}^n$ is the plant state, $\theta \in \mathbb{R}^p$ is a fixed unknown parameter vector, $u \in \mathbb{R}^m$ is the input, $y \in \mathbb{R}$ is the output, $d(t)$ is a dither signal that is typically chosen so that appropriate parameter convergence can be achieved and ξ comes from the optimization algorithm (5). The optimization

ISBN 978-1-4799-2498-1

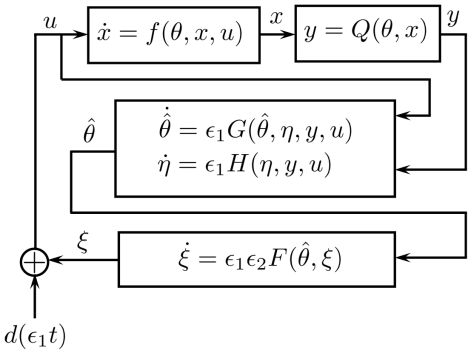

Fig. 1. The framework for grey-box ES schemes [9]

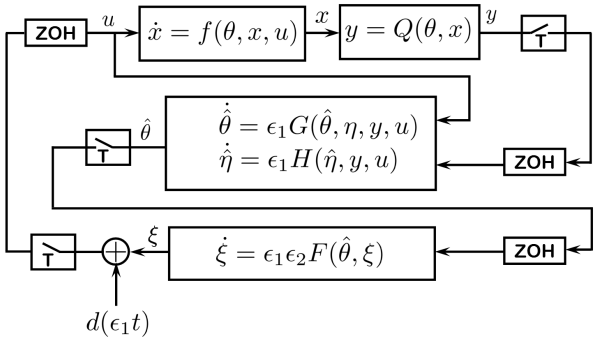

Fig. 2. Sample and zero order hold devices in the grey-box ES framework

algorithm uses the estimated parameter $\hat{\theta}$ that is obtained from the estimator (4a), (4b). The parameter estimation algorithm (4a) may contain extra states $\eta \in \mathbb{R}^q \times \mathbb{R}^s$ to widen the class of estimators considered, and ϵ_1 and ϵ_2 are tuning parameters of the estimator and optimization scheme, respectively. Note that by fine tuning ϵ_1 and ϵ_2, there are three time scales, where the plant is the fastest subsystem, $\hat{\theta}$ is the medium system and ξ is the slow system. Fig. 1 shows the relations between different parts of the closed-loop system (1)-(5).

Writing the closed loop system in coordinates $\tilde{x} := x - \ell(\theta, u), \tilde{\theta} := \hat{\theta} - \theta, \tilde{\eta} := \eta - \eta^*, \tilde{\xi} := \xi - \xi^*$ gives

$$\begin{aligned}
\dot{\tilde{x}} &= f(\theta, \tilde{x} + \ell(\theta, \tilde{\xi} + \xi^* + d(\epsilon_1 t)), \tilde{\xi} + \xi^* + d(\epsilon_1 t)) \\
&\quad -\epsilon_1 \epsilon_2 \frac{\partial \ell}{\partial u} F(\tilde{\theta} + \theta, \tilde{\xi} + \xi^*) \\
&=: \widetilde{f}(\epsilon_1 t, \tilde{x}, \tilde{\theta}, \tilde{\xi}, \epsilon_1 \epsilon_2) \qquad (6) \\
\dot{\tilde{\theta}} &= \epsilon_1\, G(\tilde{\theta} + \theta, \tilde{\eta} + \eta^*, Q(\theta, \tilde{x} + \ell(\theta, \tilde{\xi} + \xi^* + d(\epsilon_1 t))), \\
&\quad \tilde{\xi} + \xi^* + d\,(t)) \\
&=: \epsilon_1\, \widetilde{G}(\epsilon_1 t, \tilde{\eta}, \tilde{x}, \tilde{\theta}, \tilde{\xi}) \qquad (7a) \\
\dot{\tilde{\eta}} &= \epsilon_1\, H(\tilde{\eta} + \eta^*, Q(\theta, \tilde{x} + \ell(\theta, \tilde{\xi} + \xi^* + d(\epsilon_1 t))), \\
&\quad \tilde{\xi} + \xi^* + d\,(\epsilon_1 t)) \\
&=: \epsilon_1\, \widetilde{H}(\epsilon_1 t, \tilde{\eta}, \tilde{x}, \tilde{\xi}) \qquad (7b) \\
\dot{\tilde{\xi}} &= \epsilon_1\, \epsilon_2\, F(\tilde{\theta} + \theta, \tilde{\xi} + \xi^*) \\
&=: \epsilon_1\, \epsilon_2\, \widetilde{F}(\tilde{\theta}, \tilde{\xi})\ . \qquad (8)
\end{aligned}$$

where $x = \ell(\theta, u)$ is a unique solution of $0 = f(\theta, x, u)$.

Assumption 1: The continuous-time closed-loop system (1)-(5) is practically asymptotically stable uniformly in ϵ_1 and ϵ_2, i.e., there exist $\Delta > 0$ and a Lyapunov candidate $V(\tilde{x}, \tilde{\theta}, \tilde{\eta}, \tilde{\xi})$ such that for any strictly positive real number $\nu > 0$ there exist $\omega \in \mathcal{K}_\infty$ and $\epsilon_1^*, \epsilon_2^* > 0$ such that for all $\epsilon_1 \in (0, \epsilon_1^*)$ and $\epsilon_2 \in (0, \epsilon_2^*)$ the following holds:

$$\begin{aligned}
\frac{\partial V}{\partial \tilde{x}} \widetilde{f} + \frac{\partial V}{\partial \tilde{\theta}} (\epsilon_1 \widetilde{G}) + \frac{\partial V}{\partial \tilde{\eta}} (\epsilon_1 \widetilde{H}) + \frac{\partial V}{\partial \tilde{\xi}} (\epsilon_1 \epsilon_2 \widetilde{F}) \\
\leq -\omega(\tilde{x}, \tilde{\theta}, \tilde{\eta}, \tilde{\xi}) + \nu, \qquad (9)
\end{aligned}$$

for all $|\tilde{x}(t_0), \tilde{\theta}(t_0), \tilde{\eta}(t_0), \tilde{\xi}(t_0)| \leq \Delta$ and for all $t \geq t_0 \geq 0$.

Sufficient conditions under which Assumption 1 holds are presented in [9].

III. Emulation of Continuous-Time Grey-Box ES Controller

In this section, first emulation design methods are explained for the general form of the plant, parameter estimator and optimization algorithm and the consequent main result is stated. Then, the main result is applied to the particular estimator and optimizer using a particular discretization method.

A. Discrete-Time Grey-Box ES Controller

Emulation of a system consists of two steps: (1) the design of a continuous-time controller for a continuous-time plant using known continuous-time design methods to satisfy closed-loop control performance objectives, and (2) the discretization and implementation of the continuous-time controller using sample and hold devices. Fig. 2 shows the zero-order hold equivalent of the continuous time controller. Therefore, the exact discretization of the parameter estimator (7a), (7b) and optimization algorithm (8) are obtained as:

$$\begin{aligned}
\tilde{\theta}^e(k+1) &= \tilde{\theta}^e(k) \\
&\quad + \int_{kT}^{(k+1)T} \epsilon_1 \widetilde{G}(\epsilon_1 \tau, x(k), \tilde{\theta}(\tau), \tilde{\eta}(\tau), \tilde{\xi}(k)) d\tau \\
&=: \widetilde{G}_T^e(k, x(k), \tilde{\theta}(k), \tilde{\eta}(k), \tilde{\xi}(k), \epsilon_1) \qquad (10a) \\
\tilde{\eta}^e(k+1) &= \tilde{\eta}^e(k) \\
&\quad + \int_{kT}^{(k+1)T} \epsilon_1 \widetilde{H}(\epsilon_1 \tau, x(k), \tilde{\eta}(\tau), \tilde{\xi}(k)) d\tau \\
&=: \widetilde{H}_T^e(k, x(k), \tilde{\eta}(k), \tilde{\xi}(k), \epsilon_1) \qquad (10b) \\
\tilde{\xi}^e(k+1) &= \tilde{\xi}^e(k) + \int_{kT}^{(k+1)T} \epsilon_1 \epsilon_2 \widetilde{F}(\tilde{\theta}(k), \tilde{\xi}(\tau)) d\tau \\
&=: \widetilde{F}_T^e(\tilde{\theta}(k), \tilde{\xi}(k), \epsilon_1 \epsilon_2) \qquad (11)
\end{aligned}$$

where T denotes the sampling period, $\tilde{\theta}^e$, $\tilde{\eta}^e$ and $\tilde{\xi}^e$ are exact discrete values of the continuous-time states $\tilde{\theta}$, $\tilde{\eta}$ and $\tilde{\xi}$.

Due to the introduction of the new tuning parameter T and also due to the fact that, in general, it is impossible to compute $\widetilde{G}_T^e$, $\widetilde{H}_T^e$ and $\widetilde{F}_T^e$ exactly, an approximate discrete-time model of the controller should be used:

$$\begin{aligned}
\tilde{\theta}^a(k+1) &= \widetilde{G}_T^a(k, \tilde{x}(k), \tilde{\theta}(k), \tilde{\eta}(k), \tilde{\xi}(k), \epsilon_1) \qquad (12a) \\
\tilde{\eta}^a(k+1) &= \widetilde{H}_T^a(k, \tilde{x}(k), \tilde{\eta}(k), \tilde{\xi}(k), \epsilon_1) \qquad (12b)
\end{aligned}$$

$$\tilde{\xi}^a(k+1) \quad = \quad \widetilde{F}_T^a(\tilde{\theta}(k), \tilde{\xi}(k), \epsilon_1\epsilon_2) \tag{13}$$

which are obtained from (6), (7a), (7b) and (8) using one of many possible numerical integration methods (e.g. Runge-Kutta) and $\tilde{\theta}^a$, $\tilde{\eta}^a$ and $\tilde{\xi}^a$ are approximate discrete-time values of the continuous-time states $\tilde{\theta}$, $\tilde{\eta}$ and $\tilde{\xi}$.

In the ensuing sections, the discrete-time model of the plant is used which is obtained as follows:

$$\begin{aligned}\tilde{x}(k+1) \quad &= \quad \int_{kT}^{(k+1)T} \widetilde{f}(\epsilon_1\tau, \tilde{x}(\tau), \tilde{\theta}(k), \tilde{\xi}(k), \epsilon_1\epsilon_2)d\tau \\ &=: \quad \widetilde{f}_T(k, \tilde{x}(k), \tilde{\theta}(k), \tilde{\xi}(k), \epsilon_1\epsilon_2). \end{aligned} \tag{14}$$

Before stating the main result, some conditions are presented that guarantee the mismatch between the exact discrete-time model of the controller and its approximation is small.

B. Consistency Conditions

In order to guarantee that the mismatch between the exact discrete-time model of the grey-box ES controller (10a), (10b) and (11) and its approximation (12a), (12b) and (13) is small, the conditions of Assumption 1 are not enough and some form of consistency should be be considered. To this end, first one-step consistency is defined for a general non-linear continuous-time system $\dot{\psi}(t) = \Psi(\psi(t))$ and its exact and approximate discretization as $\psi^e(k+1) = \Psi_T^e(\psi^e(k))$ and $\psi^a(k+1) = \Psi_T^a(\psi^a(k))$, respectively. Then, the required condition is stated based on the consistency definition.

Definition 1: $\Psi^a(\psi^a(k))$ is one-step consistent with $\Psi^e(\psi^e(k))$ if there exist Δ such that for any $|\psi| < \Delta$, there exists T^* such that for all $T \in (0, T^*)$ the following holds:

1) Ψ_T^a is one-step consistent with $\Psi_T^{Euler} := \psi + T\Psi$, i.e., there exists a function $\rho \in \mathcal{K}_\infty$ such that:

$$|\Psi_T^a - \Psi_T^{Euler}| \leq T\rho(T)$$

2) there exist $M > 0$ and $\gamma \in \mathcal{K}_\infty$ such that for all $|\psi| < \Delta$ and $|\zeta| < \Delta$:
   - $|\Psi(\zeta)| \leq M$
   - $|\Psi(\zeta) - \Psi(\psi)| \leq \gamma(|\zeta - \psi|)$. □

Now the following assumption is considered for the exact and approximate discretization of the estimation and optimization algorithms.

Assumption 2: $\widetilde{G}_T^a(k, \tilde{x}, \tilde{\theta}, \tilde{\eta}, \tilde{\xi}, \epsilon_1)$, $\widetilde{H}_T^a(k, \tilde{x}, \tilde{\eta}, \tilde{\xi}, \epsilon_1)$ and $\widetilde{F}_T^a(\tilde{\theta}, \tilde{\xi}, \epsilon_1\epsilon_2)$ are one-step consistent with $\widetilde{G}_T^e(k, \tilde{x}, \tilde{\theta}, \tilde{\eta}, \tilde{\xi}, \epsilon_1)$, $\widetilde{H}_T^e(k, \tilde{x}, \tilde{\eta}, \tilde{\xi}, \epsilon_1)$ and $\widetilde{F}_T^e(\tilde{\theta}, \tilde{\xi}, \epsilon_1\epsilon_2)$. □

C. Main Result

Here the main result states the conditions under which the approximate discrete-time model (12a), (12b) and (13) of the continuous-time ES controller (7a), (7b) and (8) is a valid discrete-time controller for the continuous-time plant (6) and preserves stability property of the continuous-time controller under sampling.

Theorem 1: Suppose that Assumptions 1 and 2 hold. Let Δ come from Assumption 1 and $\widehat{\nu}$ be given. Then, for any $\widehat{\nu} > 0$ there exist $\epsilon_1^*, \epsilon_2^*$ such that for any fixed $\epsilon_1 \in (0, \epsilon_1^*)$, $\epsilon_2 \in (0, \epsilon_2^*)$ there exists T^* such that for all $T \in (0, T^*)$, the following holds for the approximate discrete-time closed-loop system (12a)-(14):

$$\begin{aligned}\frac{\Delta V}{T} &= \frac{V(\tilde{x}(k+1), \tilde{\theta}(k+1), \tilde{\eta}(k+1), \tilde{\xi}(k+1))}{T} \\ &- \frac{V(\tilde{x}(k), \tilde{\theta}(k), \tilde{\eta}(k), \tilde{\xi}(k))}{T} \leq -\omega(\tilde{x}, \tilde{\theta}, \tilde{\eta}, \tilde{\xi}) + \widehat{\nu} \end{aligned} \tag{15}$$

for all $|(\tilde{x}_0, \tilde{\theta}_0, \tilde{\eta}_0, \tilde{\xi}_0)| \leq \Delta$ and all $k \geq 0$.

Proof: See Appendix.

Remark 1: The property (15) guarantees practical asymptotic stability of the closed-loop system (12a)-(14).

Remark 2: The tuning procedure according to Theorem 1 is as follows. For any desired accuracy of the approximate discrete-time closed-loop system (12a)-(14) characterized by $\widehat{\nu}$, first the parameters ϵ_1 and ϵ_2 are adjusted to deliver appropriate convergence of the continuous-time scheme. Then the sample period T should be tuned so that for all initial conditions in the ball $\mathcal{B}_\Delta$:

- The system state x converges to the $\mathcal{B}_{\widehat{\nu}}$ ball centered at the equilibrium point of the plant in time scale kT;
- The parameter estimate $\hat{\theta}$ converges to the $\mathcal{B}_{\widehat{\nu}}$ ball centered at the true value of the parameter θ in the slower time scale $\epsilon_1 kT$;
- The optimizer state ξ converges in the slowest time scale $\epsilon_1\epsilon_2 kT$ to the $\mathcal{B}_{\widehat{\nu}}$ ball centered at the optimal value ξ^*.

Remark 3: The approximate discrete-time controller recovers the performance of the continuous-time controller as sample period becomes sufficiently small, i.e. $\mathcal{B}_{\widehat{\nu}} \to \mathcal{B}_\nu$ as $T \to 0$.

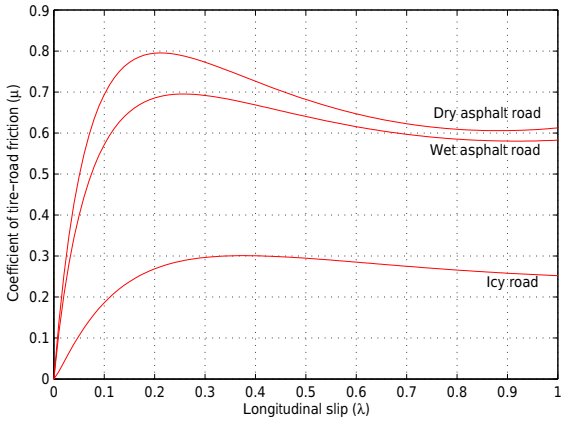

Fig. 3. Friction force coefficient $\mu(\lambda)$ in different road conditions

IV. Applications of the Main Result

In this section the discrete-time implementation of the grey-box ES controller is illustrated by simulation of a Anti-lock Braking System (ABS) through simulations and real implementation of an online calibration routine for spark timing optimization.

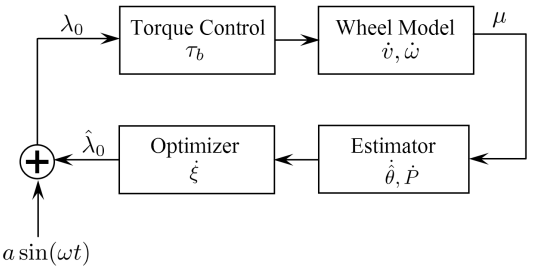

Fig. 4. Grey-box extremum seeking scheme for the ABS problem

A. Application to Anti-lock Braking System

The ABS design objective is to regulate the wheel longitudinal slip (λ) to the maximum point of the friction curve in any road conditions (Fig. 3) in order to generate the maximum braking force. To this end, a continuous-time ES controller is used from [9] which satisfies Assumption 1. Then, using recursive least-squares algorithm for estimator and Jacobian matrix transpose for optimizer, the equations of the ABS problem are as follows:

$$\dot{\lambda} = -c(\lambda - \lambda_0) = f(\lambda, \lambda_0), \quad (16)$$

$$y = \phi^T(\lambda)\theta = h(\theta, \lambda), \quad (17)$$

$$\dot{\hat{\theta}} = -\epsilon_1 P\phi(y - \phi^T\hat{\theta}) = \epsilon_1 G(\lambda, \hat{\theta}, P, \xi) \quad (18)$$

$$\dot{P} = \epsilon_1(\gamma P - P\phi\phi^T P) = \epsilon_1 H(\lambda, P, \xi) \quad (19)$$

$$\begin{aligned}\dot{\xi} &= -\epsilon_1\epsilon_2\Gamma J_r^T(\xi)\nabla h(\xi) = -\epsilon_1\epsilon_2\Gamma\left(\frac{\hat{p}_3}{\xi} - \frac{\hat{p}_4}{\xi^2}\right) \\ &\quad \times\left(-\hat{p}_2 + \hat{p}_3(ln\xi + 1) + \hat{p}_4(\frac{1}{\xi})\right) \\ &= \epsilon_1\epsilon_2 F(\hat{\theta}, \xi)\ , \end{aligned} \quad (20)$$

where $\lambda = (v - R\omega)/v$, v is the longitudinal speed of the vehicle, R the radius of the wheel, ω the angular velocity, λ_0 is the control input, $\lambda_0 = \xi + d(t)$, $\phi = [1, -\lambda, \lambda ln\lambda, ln\lambda, -v]$, $\theta = [p_1, p_2, p_3, p_4, p_5]$ is the vector of unknown parameters to be estimated, $\gamma \geq 0$, P is the error covariance matrix, $\nabla h(\xi)$ denotes the gradient of h at ξ, J_r represents the Jacobian of $r(\xi) = \nabla h(\xi)$ and Γ is an arbitrary positive definite matrix. In addition, it is assumed that $\xi^* \neq \frac{p_4}{p_3}$ and $d(t) = 0.02\sin(9t)$.

Writing (18)-(20) in coordinates $\tilde{\theta} = \hat{\theta} - \theta$ and $\tilde{\xi} = \xi - \xi^*$, the continuous-time ES controller can be expressed in the form:

$$\dot{\tilde{\theta}} = \epsilon_1\widetilde{G}(\tilde{\theta}, \tilde{\xi}) \quad (21)$$

$$\dot{P} = \epsilon_1\widetilde{H}(P, \tilde{\xi}) \quad (22)$$

$$\dot{\tilde{\xi}} = \epsilon_1\epsilon_2\widetilde{F}(\tilde{\theta}, \tilde{\xi}) \quad (23)$$

Now, to verify Assumption 2, the second order Runge-Kutta method is employed to state an approximate discrete-time model of the continuous-time controller (21)-(23) as $\widetilde{G}_T^a$ and $\widetilde{F}_T^a$. Then, $\widetilde{G}_T^a$ satisfies Assumption 2 because $\widetilde{G}_T^a$ is one-step consistent with $\widetilde{G}_T^{Euler}$ with $\rho_1(s) = s$, $\widetilde{G}$ and its derivative w.r.t $\tilde{\theta}$ are bounded. Assumption 2 holds for $\widetilde{F}_T^a$ since $\widetilde{F}_T^a$ is one-step consistent with $\widetilde{F}_T^{Euler}$ with $\rho_2(s) = s^2$, $\widetilde{F}$ and its derivative w.r.t $\tilde{\xi}$ are bounded. Therefore, all assumptions of Theorem 1 hold.

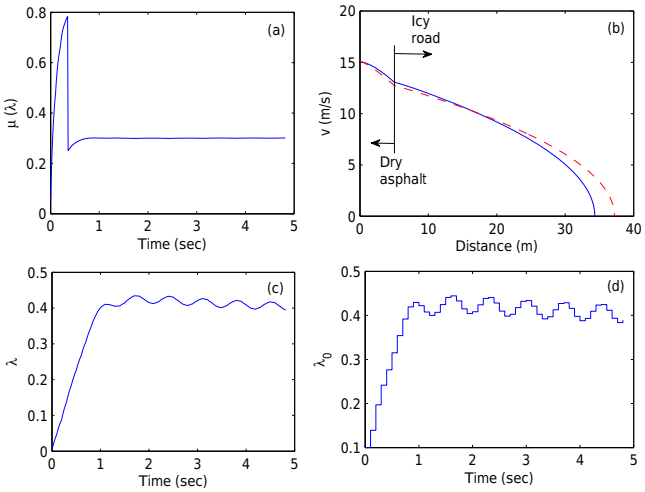

Fig. 5. ABS design using Discrete-time ES controller; (a) Performance output (friction force coefficient), (b) Stop distance (dashed-line shows the case that extremum seeking scheme is not utilized and λ^* of dry asphalt road in used for the whole road), (c) State (longitudinal slip) , (d) Control input (desired longitudinal slip).

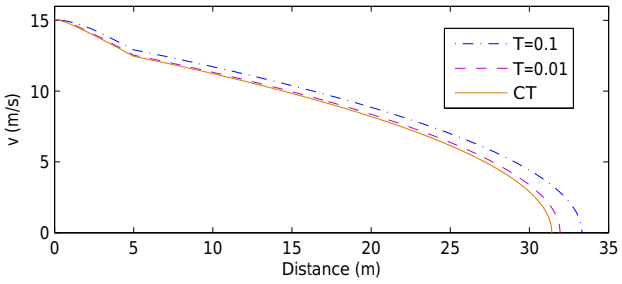

Fig. 6. Comparing performance of emulated ES controller in different sample rates with continuous-time (CT) ES controller

For simulation purposes, the initial conditions are $v(0) = 15m/s$ and $\omega(0) = 111.11$, which makes $\lambda(0) = 0$ and $\hat{\lambda}_0(0) = 0.1$. The unknown parameters are initialized at $\hat{\theta}(0) = [3.16, 3.3, 2.64, 1.05, 0.01]$, identical to those in [15] The sampling period is $T = 0.1$. It is assumed that the braking starts on a dry asphalt road and after $5m$ the road becomes icy. The ES scheme estimates optimal value of λ_0 in different road conditions and then drive λ_0 to its optimal value λ_0^* so that friction coefficient converges to its maximum point at each road condition.

The simulation results in Fig. 5 (solid curves) show that during braking, friction coefficients approach their maximum values on dry asphalt road ($\mu^* = 0.8$) and icy road ($\mu^* = 0.3$) and the vehicle stopped within the shortest distance ($33.3m$). The dashed-curve in Fig. 5 shows the case that λ^* of dry asphalt road in used for the whole road. In this case, the vehicle stops after $37.2m$. In addition, Fig. 6 shows that the emulated ES controller recovers the performance of the continuous-time controller (17)-(20) as $T \to 0$ validating

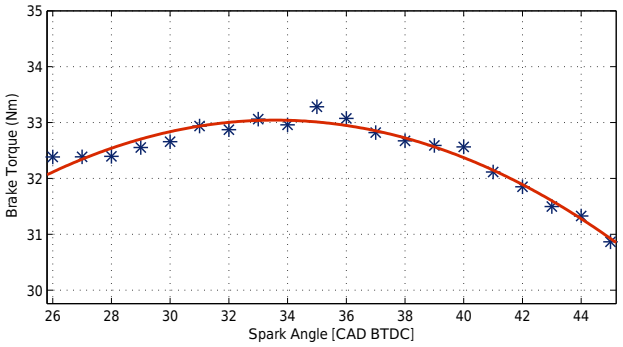

Fig. 7. Steady-state mapping between the spark angle and brake torque at 800rmp and 30Nm - CAD BTDC means Crank Angle Degrees Before Top-Dead Center

Remark 3.

B. Application to Spark timing Calibration

Spark timing is an important parameter in engine performance and emissions. The objective of spark timing (spark angle) control is to find the crank angle position where the mixture of air and fuel in compression stroke should be ignited to produce the maximum brake torque (MBT), called MBT spark timing. The main advantage of using ES controller is that it can reduce the calibration time and effort as proposed in [12]. In addition, ES methods have been proposed for varying conditions such as fuel composition variations in flex-fuel engines which affects the MBT spark timing [4], [7].

The experiments are carried out in a six cylinder, 4L Ford Falcon BF MY2006 engine converted for natural gas and connected to an eddy current type dynamometer. The experiments were performed at the engine operating conditions of 800rpm, 30Nm, and stoichiometric air/fuel ratio. The engine was controlled using ATI Vision software. ATI mapped fragments of the engine control unit (ECU) memory to symbolic names, which could be read or written to during engine operation as required. ATI was also connected to various data acquisition cards, enabling the logging of external sensor outputs. In order to measure the brake torque, the outputs from a strain gauge installed on dynamometer, are converted into voltage signals and read by the DAQ. In addition, an application programming interface (API) was developed in ATI to communicate with MATLAB, which was the host language for the ES controller.

In order to apply the grey-box ES controller to adjust the spark advance, a parameterized model of the mapping between the spark advance and the brake torque is required. In Fig. 7, using some open-loop tests, it is shown that this parameterized model is well represented by a quadratic function; i.e.:

$$\tau = a\alpha_{sa}^2 + b\alpha_{sa} + c = h(\theta, \alpha_{sa}) \quad (24)$$

where τ is the engine brake torque, α_{sa} is the spark angle, $\theta = [a\ b\ c]^T$ is the unknown parameter vector and a, b, c are unknown, nominally constant parameters for a given fuel

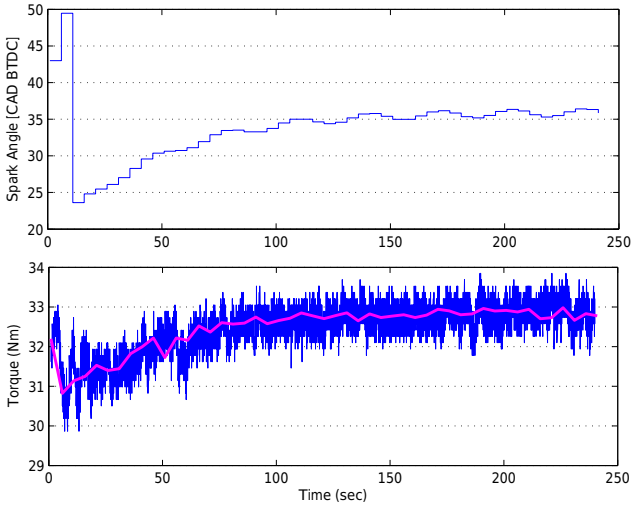

Fig. 8. Grey-box ES controller performance for the spark timing calibration

composition. By introducing $\phi = [\alpha_{sa}^2\ \alpha_{sa}\ 1]^T$, (24) can be written in the following compact form:

$$\tau = \phi^T(\alpha_{sa})\theta \quad (25)$$

The fitted curve in Fig. 7 correspond to the set of values for $\theta^T = [a\ \ b\ \ c]$ as $\theta^T = [-0.016\ \ 1.15\ \ -5.4]$. This set of parameters are obtained via fitting quadratic curves to the mappings of Fig. 7. Note that we do not assume *a priori* knowledge neither about true values of parameters nor extremum value of the spark timing. The purpose of grey-box ES controller is to manipulate α_{sa} to optimize τ and consequently maximize efficiency.

Using recursive least-squares algorithm for estimator and gradient method for optimizer, the problem formulation for the spark angle control is:

$$y = \phi^T(\alpha_{sa})\theta = h(\theta, \alpha_{sa}), \quad (26)$$
$$\dot{\hat{\theta}} = -P\phi(y - \phi^T\hat{\theta}) = G(\hat{\theta}, P, \xi) \quad (27)$$
$$\dot{P} = \gamma P - P\phi\phi^T P = H(P, \xi) \quad (28)$$
$$\dot{\xi} = -\epsilon\Gamma\nabla h(\xi) = -\epsilon\Gamma(2a\xi + b) = \epsilon F(\hat{\theta}, \xi)\ , \quad (29)$$

Now assumptions of Theorem 1 can be verified. According to [9], Assumption 1 holds for (26)-(29) if the vector $\phi(\alpha_{sa})$ in (25) satisfies persistency of excitation (PE) condition. This condition holds with dither signal $d(t) = \sin(t)$. To verify Assumption 2, the Euler method is used to discretize the continuous-time controller (27)-(29) which provides discrete-time model of the controller as $\widetilde{G}_T^a$, $\widetilde{H}_T^a$ and $\widetilde{F}_T^a$. Then, regarding Definition 1:

- $\widetilde{G}_T^a$, $\widetilde{H}_T^a$ and $\widetilde{F}_T^a$ are obviously one-step consistent with $\widetilde{G}_T^{Euler}$, $\widetilde{H}_T^{Euler}$ and $\widetilde{F}_T^{Euler}$ as Euler method is used for discretization,
- $\widetilde{G}$, $\widetilde{H}$ and $\widetilde{F}$ are upper bounded and derivatives of $\widetilde{G}$ w.r.t $\tilde{\theta}$, $\widetilde{H}$ w.r.t $\widetilde{P}$ and $\widetilde{F}$ w.r.t $\tilde{\xi}$ are bounded.

Therefore, all assumptions of Theorem 1 hold.

The designed discrete-time grey-box ES controller was tested at the engine operating point of 800rpm and 30Nm.

For each iteration of the controller, the ES algorithm waits for two seconds after changing spark angle, then averages the brake torque signal for three seconds. The ES perturbation frequency and amplitude are $\omega = 1$ and $a = 0.3$. The initial conditions are $\alpha_{sa}(0) = \xi(0) = 42$, $\theta(0) = [0.0015\ 0.13\ 6]$, and $P(0) = 100I$.

Fig. 8 shows that the spark angle converges to its optimum value at $\alpha^*_{sa} = 35$ CAD BTDC in 100 seconds. As depicted in Fig. 8 after convergence to optimum spark advance it is still oscillating around the optimum value due to the dither signal required for the parameter estimation. Any loss due to the dither oscillations after convergence is masked by cyclic variations in brake torque.

V. Conclusion

In this paper, the emulation design was developed for the grey-box of ES controllers. The design uses the continuous-time ES controller which satisfies certain stability conditions and discretize it using sample and hold devices. The conditions under which the designed discrete-time ES controller can be implemented to control of the continuous-time plant are presented. The ABS problem and spark timing calibration are also used to illustrate the proposed design method.

Appendix
Proof of Theorem 1

The proof of Theorem 1 follows the same steps as that of Theorem 3.1 in [5]. The only difference is that here we have two tuning parameters, ϵ_1 and ϵ_2, that should be included in the conditions for obtaining T^*.

Let a 8-tuple of strictly real numbers $(\Delta_{\tilde{x}}, \Delta_{\tilde{\theta}}, \Delta_{\tilde{\eta}}, \Delta_{\tilde{\eta}}, \Delta_d, \Delta_{\dot{d}}, \hat{\nu}, \nu)$ be given. Let these data generate $\rho_1, \rho_2 \in \mathcal{K}_\infty$ from the definition of the one-step consistency. Define $\mathcal{R}_{\tilde{x}} := \Delta_{\tilde{x}} + 1$, $\mathcal{R}_{\tilde{\theta}} := \Delta_{\tilde{\theta}} + 1$, $\mathcal{R}_{\tilde{\eta}} := \Delta_{\tilde{\eta}} + 1$ and $\mathcal{R}_{\tilde{\xi}} := \Delta_{\tilde{\xi}} + 1$. Let $L > 0$ be the Lipschitz constant of $\widetilde{f}$, $\widetilde{G}$, $\widetilde{H}$ and $\widetilde{F}$ on the sets where $|\tilde{x}| \leq \mathcal{R}_{\tilde{x}}$, $|\tilde{\theta}| \leq \mathcal{R}_{\tilde{\theta}}$, $|\tilde{\eta}| \leq \mathcal{R}_{\tilde{\eta}}$, $|\tilde{\xi}| \leq \mathcal{R}_{\tilde{\xi}}$, $|d| \leq \Delta_d$. Let $b > 0$ be a number that satisfies $\max\left\{|\frac{\partial V}{\partial \tilde{x}}|, \left|\frac{\partial V}{\partial \tilde{\theta}}\right|, \left|\frac{\partial V}{\partial \tilde{\eta}}\right|, \left|\frac{\partial V}{\partial \tilde{\xi}}\right|, |\widetilde{f}|, |\widetilde{G}|, |\widetilde{H}|, |\widetilde{F}|\right\} \leq b$ for all $\tilde{x} \leq \mathcal{R}_{\tilde{x}}$, $\tilde{\theta} \leq \mathcal{R}_{\tilde{\theta}}$, $\tilde{\eta} \leq \mathcal{R}_{\tilde{\eta}}$, $\tilde{\xi} \leq \mathcal{R}_{\tilde{\xi}}$, $d \leq \Delta_d$. Define $\Delta := \Delta_{\tilde{x}} + \Delta_{\tilde{\theta}} + \Delta_{\tilde{\eta}} + \Delta_{\tilde{\xi}} + \Delta_d$.

It is assumed without loss of generality that $\hat{\nu} \leq 1$ and $b \geq 1$ and define

$$T^*_1 := \min\left\{\frac{1}{4b}, \rho_1^{-1}\left(\frac{\hat{\nu}}{4b}\right), \rho_2^{-1}\left(\frac{\hat{\nu}}{4b}\right)\right\}$$

Note that $T^*_1 \leq \frac{1}{4b} \leq \frac{1}{4} < 1$.

Let $T^*_2 > 0$ be such that $\forall T \in (0, T^*_2)$ the following holds:

$$\epsilon^*_1 bL\left[(\Delta+1)\frac{\exp(LT) - 1 - LT}{LT} + \frac{1}{2}\Delta_{\dot{d}} T\right] \leq \frac{\hat{\nu}}{32}$$

Let $T^*_3 > 0$ be such that $\forall T \in (0, T^*_3)$ the following holds:

$$\epsilon^*_1\epsilon^*_2 bL\left[(\Delta+1)\frac{\exp(LT) - 1 - LT}{LT} + \frac{1}{2}\Delta_{\dot{d}} T\right] \leq \frac{\hat{\nu}}{32}$$

Let $\tilde{x}_1 := \widetilde{f} + \gamma_1 T\widetilde{f}$, $\tilde{\theta}_1 := \tilde{\theta} + \gamma_2 T\widetilde{G}$, $\tilde{\eta}_1 := \tilde{\eta} + \gamma_3 T\widetilde{H}$, $\tilde{\xi}_1 := \tilde{\xi} + \gamma_4 T\widetilde{F}$ where $\gamma_1, \gamma_2, \gamma_3, \gamma_4 \in (0, 1)$.

Let $T^*_4 > 0$, $T^*_5 > 0$, $T^*_6 > 0$ and $T^*_7 > 0$ such that:

$$b\left|\frac{\partial V}{\partial \tilde{x}}|_{(\tilde{x}_1, \tilde{\theta}+T\epsilon_1\widetilde{G}, \tilde{\eta}+T\epsilon_1\widetilde{H}, \tilde{\xi}+T\epsilon_1\epsilon_2\widetilde{F})} - \frac{\partial V}{\partial \tilde{x}}|_{(\tilde{x},\tilde{\theta},\tilde{\eta},\tilde{\xi})}\right| \leq \frac{\hat{\nu}}{32}, \qquad \forall T \in (0, T^*_4)$$

$$\epsilon^*_1 b\left|\frac{\partial V}{\partial x_m}|_{(\tilde{x}, \tilde{\theta}_1, \tilde{\eta}+T\epsilon_1\widetilde{H}, \tilde{\xi}+T\epsilon_1\epsilon_2\widetilde{F})} - \frac{\partial V}{\partial x_m}|_{(\tilde{x},\tilde{\theta},\tilde{\eta},\tilde{\xi})}\right| \leq \frac{\hat{\nu}}{32}, \qquad \forall T \in (0, T^*_5)$$

$$\epsilon^*_1 b\left|\frac{\partial V}{\partial x_m}|_{(\tilde{x}, \tilde{\theta}, \tilde{\eta}_1, \tilde{\xi}+T\epsilon_1\epsilon_2\widetilde{F})} - \frac{\partial V}{\partial x_m}|_{(\tilde{x},\tilde{\theta},\tilde{\eta},\tilde{\xi})}\right| \leq \frac{\hat{\nu}}{32}, \qquad \forall T \in (0, T^*_6)$$

$$\epsilon^*_1\epsilon^*_2 b\left|\frac{\partial V}{\partial x_s}|_{(\tilde{x},\tilde{\theta},\tilde{\eta},\tilde{\xi}_1)} - \frac{\partial V}{\partial x_s}|_{(\tilde{x},\tilde{\theta},\tilde{\eta},\tilde{\xi})}\right| \leq \frac{\hat{\nu}}{32}, \quad \forall T \in (0, T^*_7)$$

for all T^*_4, T^*_5, T^*_6 and T^*_7. Finally, we define

$$T^* := \min\{T^*_1, T^*_2, T^*_3, T^*_4, T^*_5, T^*_6, T^*_7\}.$$

Considering conditions above, the rest of proof follows the same steps of [5].

References

[1] Adetola, V. and Guay, M., "Integration of real-time optimization and model predictive control," Journal of Process Control vol. 20, 2010, pp. 125–133.

[2] Ariyur, K. B. and Krstić, M., *Real-Time Optimization by Extremum-Seeking Control*, Wiley-Interscience, A John Wiley & Sons, Inc., Publication, 2003.

[3] Choi, J. Y., Krstić, M., Ariyur, K. B. and Lee, J. S., Extremum seeking control for discrete-time systems, *IEEE Trans. Automat. Contr.*, vol. 47, pp. 318-23, 2002.

[4] Hellstrom, E., Lee, D., Jiang, l., Stefanopoulou, A. G. and Yilmaz, H., On-Board Calibration of Spark Timing by Extremum Seeking for Flex-Fuel Engines, *IEEE Transactions on Control Systems Technology*, DOI:10.1109/TCST.2012.2236093, 2013.

[5] Laila, D. S. and Nešić, "Open-and closed-loop dissipation inequalities under sampling and controller emulation", *European Journal of Control*, vol. 8, No. 2, pp. 109-125, 2002.

[6] Manzie, C. and Krstić, M., Extremum Seeking With Stochastic Perturbations, *IEEE Trans. Automat. Contr.*, vol. 54, pp. 580-85, 2009.

[7] Mohammadi, A., Nešić, D. and Manzie, C., "Extremum Seeking Methods for Online Optimization of Spark Advance in Alternative Fueled Engines", Proceedings of *Engine and Powertrain Control, Simulation and Modeling*, Vol. 3, No. 1, pp. 1-8, 2012.

[8] Nešić, D., "Extremum seeking control: convergence analysis", *Europ. J. Contr.*, vol. 15, No. 3-4, pp. 331-347, 2009.

[9] Nešić, D., Mohammadi, A. and Manzie, C., "A Framework for Extremum Seeking Control of Systems with Parameter Uncertainties", *IEEE Trans. Automat. Contr.*, Vol.58, Issue 2, pp.435-448, 2013.

[10] Nešić, D., Teel, A. R. and Kokotović, P. V. "Sufficient conditions for stabilization of sampled-data nonlinear systems via discrete-time approximations", *Systems & Control Letters*, Vol. 8, Issues 4-5, pp. 259-270, 1999.

[11] Pierre, D. A. and Pierre, J. W., "Digital controller design - Alternative emulation approaches", *ISA Transactions*, vol. 34, pp. 219-28, 1995.

[12] Popović, D., Janković, M., Magner, S. and Teel, A. R. "Extremum Seeking Methods for Optimization of Variable Cam Timimg Engine Operation", *IEEE Trans. on Contr. Sys. Tech.*, vol. 14, No. 3, 2006, pp. 398-407.

[13] Qu, Z., *Robust control of nonlinear uncertain systems*, John Wiley & Sons: New York, 1998.

[14] Teel, A. R., Nešić, D. and Kokotović, P. V. "A note on input-to-state stability of sampled-data nonlinear systems", Proceedings of *37th IEEE Conference on Decision and Control*, 1998.

[15] Yi, J., Alvarez, L. and Horowitz, R., "Adaptive Emergency Braking Control With Underestimation of Friction Coefficient ", *IEEE Trans. on Contr. Sys. Tech.*, vol. 10, No. 3, pp. 381-92, 1992.